Dark matter in the new bulk region of the MSSM

Patrick Stengel

University of Michigan

May 19, 2017

1705.maybe with Andrew Davidson,
Chris Kelso, Jason Kumar and Pearl Sandick
1706.????? with Bhaskar Dutta, Kebur Fantahun, Ashen Fernando,
Tathagata Ghosh, Jason Kumar, Pearl Sandick and Joel Walker

Outline

Typical mSUGRA/CMSSM scenario with $\widetilde{B}$-$\widetilde{H}$ admixture

Relic density with $\bar{\chi}\chi \to WW, ff$

- Assuming gaugino mass unification (at least $M_1 \lesssim M_2$), yields neutralino with small $\widetilde{W}$
- Minimal flavor violation eliminates sfermion mixing
- Need $\mu/m_\chi \sim \mathcal{O}(1)$ for s-wave

see e.g. Feng, Sanford 1009.3934

SI scattering with Higgs exchange

- Scalar mediated interactions are velocity independent
- Minimal flavor violation guarantees coupling $\sim m_q$
- LHC data and $m_h \simeq 125\,\mathrm{GeV}$ push unified $m_{\tilde{f}} \gtrsim \mathcal{O}(\,\mathrm{TeV})$

see e.g. Baer et. al. 1112.3017

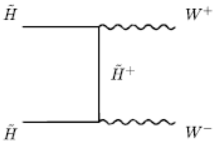

(a)Chargino-mediated Annihilation to W^+W^-

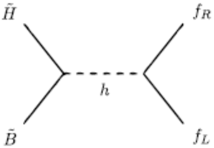

(c)Higgs-mediated Annihilation to Fermions

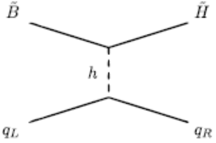

(a)Higgs-mediated Scattering

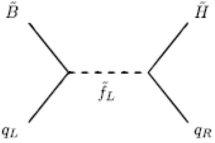

(b)Squark-mediated Scattering

Resurrect "bulk" region by relaxing MFV, allowing light $\tilde{f}$

Light flavor squark co-annihilation

- Pure $\widetilde{B}$ need sfermions with L-R mixing, nondegenerate masses for s-wave annihilation
- LHC less sensitive for $m_\chi \simeq m_{\tilde{q}} \gtrsim \mathcal{O}(200\,\mathrm{GeV})$
- Need $\tilde{q}^*\tilde{q} \to gg$, $\chi\tilde{q} \to gq$

Scattering through squark exchange

- Enhanced scattering cross section for $m_\chi \simeq m_{\tilde{q}}$
- Need small mixing angle for consistency with LUX data
- Velocity/spin-dependent contributions can dominate

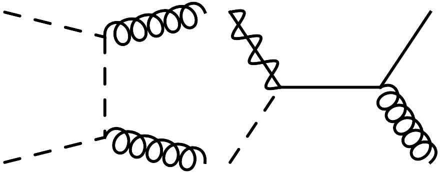

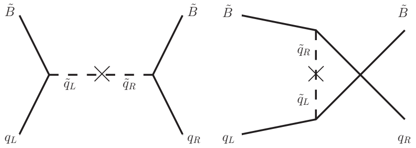

Squark mass limits from jets + MET searches

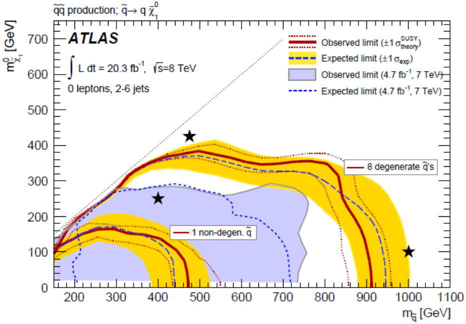

Figure: Simplified models only considering production of light flavor squark pairs, see *ATLAS 1405.7875*

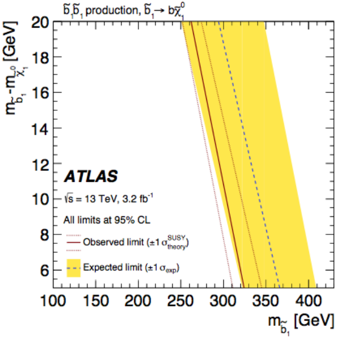

Figure: Use ISR to boost MET and help identify signal events, *ATLAS 1604.07773*

"Simplified" model with singlet DM, squark mediator(s)

$$\mathcal{L}_{int} = \sum_{q=u,d,s} \lambda_{Lq}(\bar{\chi}P_L q)\tilde{q}_L^* + \lambda_{Rq}(\bar{\chi}P_R q)\tilde{q}_R^* + h.c.$$

$$\tilde{q}_L = \tilde{q}_1 \cos\alpha + \tilde{q}_2 \sin\alpha$$

$$\tilde{q}_R = -\tilde{q}_1 \sin\alpha + \tilde{q}_2 \cos\alpha$$

Gauge invariance requires squark couplings to SM gauge bosons

$$\langle \sigma v(\tilde{q}^*\tilde{q} \to gg)\rangle = \frac{7 g_s^4 N_{\tilde{q}}}{432\pi m_{\tilde{q}}^2}\left[N_{\tilde{q}} + \frac{\exp\left(\Delta m/T\right)}{3\left(1+\Delta m/m_\chi\right)^{3/2}}\right]^{-2}$$

- For small $\Delta m = m_{\tilde{q}} - m_\chi$, QCD processes dominate annihilation
- Temperature at freeze out $T \simeq m_\chi/25$ for correct relic density
- Sum over $N_{\tilde{q}}$ mass degenerate light flavor squarks species

Co-annihilation processes needed to deplete relic desity

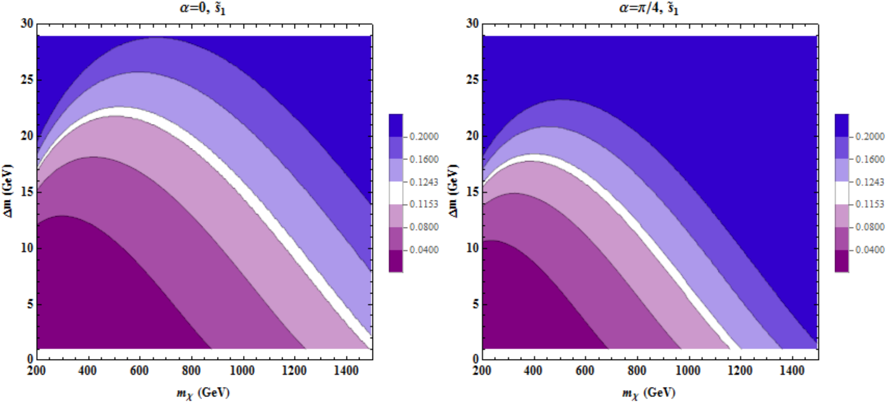

Figure: Relic density contours for benchmarks with a light d/s-type squark.

Adding squarks can raise or lower *effective* $\langle \sigma v \rangle$

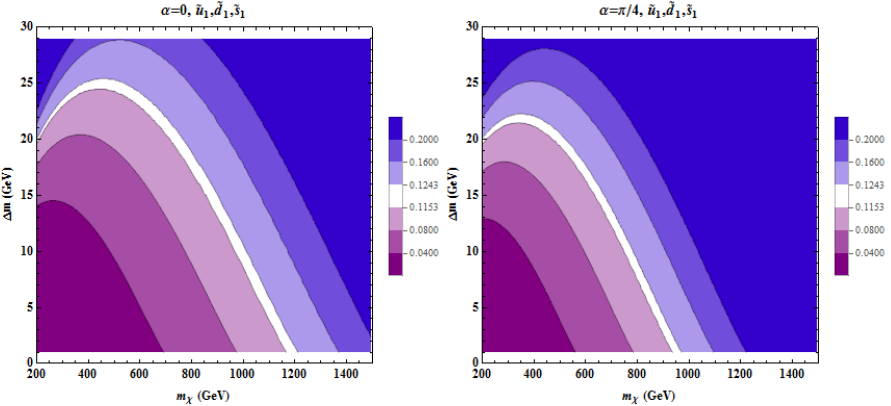

Figure: Relic density contours for benchmarks with light u-, d- and s-type squarks.

CP-even operators for squark exchange with $m_{\tilde{q}_1} \ll m_{\tilde{q}_2}$

$$\mathcal{O}_{q1} = \alpha_{q1}(\bar{\chi}\gamma^\mu\gamma^5\chi)(\bar{q}\gamma_\mu q)$$
$$\mathcal{O}_{q2} = \alpha_{q2}(\bar{\chi}\gamma^\mu\gamma^5\chi)(\bar{q}\gamma_\mu\gamma^5 q)$$
$$\mathcal{O}_{q3} = \alpha_{q3}(\bar{\chi}\chi)(\bar{q}q)$$
$$\mathcal{O}_{q4} = \alpha_{q4}(\bar{\chi}\gamma^5\chi)(\bar{q}\gamma^5 q)$$

Scattering enhanced $m_\chi \simeq m_{\tilde{q}_1}$

- $\mathcal{O}_{q1,3}$ spin independent
- $\mathcal{O}_{q2,4}$ spin dependent
- $\mathcal{O}_{q2,3}$ velocity independent

$$\alpha_{q1} = -\left[\frac{|\lambda_L^2|}{8}\left(\frac{\cos^2\alpha}{m_{\tilde{q}_1}^2 - m_\chi^2}\right) - \frac{|\lambda_R^2|}{8}\left(\frac{\sin^2\alpha}{m_{\tilde{q}_1}^2 - m_\chi^2}\right)\right]$$

$$\alpha_{q2} = \left[\frac{|\lambda_L^2|}{8}\left(\frac{\cos^2\alpha}{m_{\tilde{q}_1}^2 - m_\chi^2}\right) + \frac{|\lambda_R^2|}{8}\left(\frac{\sin^2\alpha}{m_{\tilde{q}_1}^2 - m_\chi^2}\right)\right]$$

$$\alpha_{q3,4} = \frac{Re(\lambda_L\lambda_R^*)}{4}(\cos\alpha\sin\alpha)\left[\frac{1}{m_{\tilde{q}_1}^2 - m_\chi^2}\right]$$

$\alpha^2 \ll 1$ can surpress $\mathcal{O}_{q3}$ more than v^2 in $\mathcal{O}_{q1}$, A^{-2} in $\mathcal{O}_{q2}$

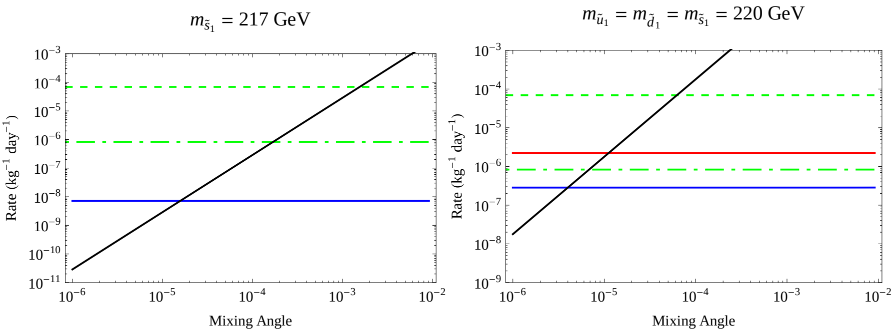

Figure: Event rate in Xenon-based detector as a function of α for $\mathcal{O}_{q1}$, $\mathcal{O}_{q2}$, $\mathcal{O}_{q3}$, $m_\chi = 200\,\mathrm{GeV}$. Also show limits from LUX (dashed) and projections from LZ-7 (dash-dotted).

Sensitivity of direct detection to SI scattering

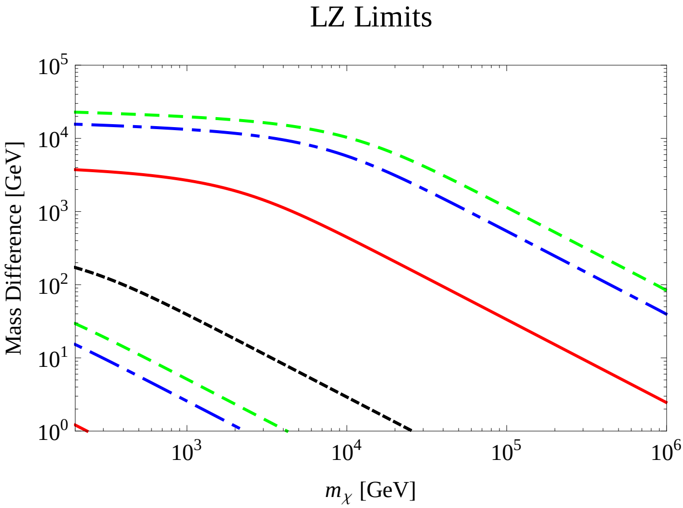

Figure: Projected LZ-7 sensitivity for benchmarks $\tilde{u}_1$, $\tilde{s}_1$, $\tilde{u}_1\tilde{d}_1\tilde{s}_1$, $\tilde{u}_1\tilde{u}_2$.

Outline

Can also satisfy relic density with *L*-*R* slepton mixing

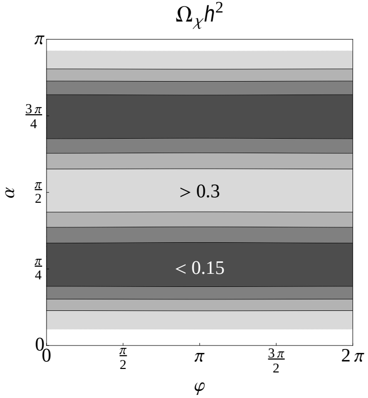

Figure: Bino relic abundance assuming smuon mixing with $m_\chi = 100\,\mathrm{GeV}$, $m_{\tilde{\mu}_1} = 120\,\mathrm{GeV}$ and $m_{\tilde{\mu}_2} = 300\,\mathrm{GeV}$.

$$\begin{aligned}
\mathcal{L}_{int} &= \lambda_L \tilde{\ell}_L \bar{\chi} P_L \ell + \lambda_R \tilde{\ell}_R \bar{\chi} P_R \ell \\
&\quad + \lambda_L^* \tilde{\ell}_L^* \bar{\chi} P_L l + \lambda_R^* \tilde{\ell}_R^* \bar{\chi} P_R \ell \\
\lambda_L &= \sqrt{2} g Y_L e^{\imath\phi/2} \\
\lambda_R &= \sqrt{2} g Y_R e^{-\imath\phi/2} \\
\begin{bmatrix} \tilde{\ell}_1 \\ \tilde{\ell}_2 \end{bmatrix} &= \begin{bmatrix} \cos\alpha & -\sin\alpha \\ \sin\alpha & \cos\alpha \end{bmatrix} \begin{bmatrix} \tilde{\ell}_L \\ \tilde{\ell}_R \end{bmatrix}
\end{aligned}$$

L-R mixing angle α, CP-violating phase ϕ

Dipole moments constrain mixing

Rule out $\tilde{e}$, constrain $\tilde{\mu}$, allow $\tilde{\tau}$

Can use ISR to boost MET and help S-B discrimination

$\tilde{\mu}_L$ with $30\,\mathrm{GeV} < \Delta m < 60\,\mathrm{GeV}$

- Can generally satisfy relic density with bino DM
- Do not need monojet for $\Delta m \gtrsim 70\,\mathrm{GeV}$
- Look for OSSF muons, one hard non-b jet and MET

Basic cuts reduce SM background

- $t\bar{t}$ needs one missed jet, both mistagged
- $Z \to \tau\bar{\tau} \to \ell^+\ell^- + 4\nu$ reduced by $M_{\tau\tau} > 175\,\mathrm{GeV}$

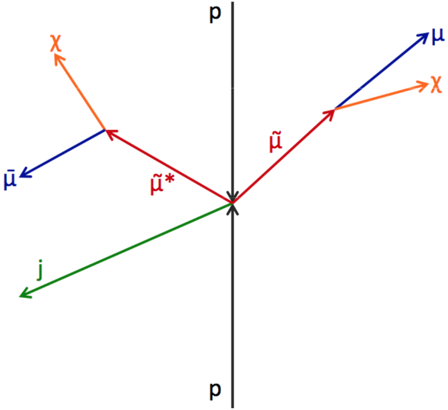

Angular variables can help reduce remaining backgrounds

Decay products collimated for parents produced above threshold

- $ZZ \to \ell^+\ell^-\nu\bar{\nu}$ leptons collimated, anti-collimated $\not{E}_T$
- $W^+W^- \to \ell^+\nu\ell^-\bar{\nu}$ leptons anti-collimated, collimated $\not{E}_T$

WW leptons, MET look like signal

- ISR boost smears collimation, $p_T(j)$ cut cannot be too high
- Less smearing for heavier parents, use rapidity to distinguish parent spin

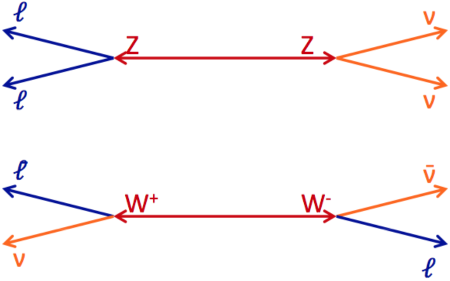

Figure: Credit J. Kumar

For $p_T(\ell) \ll p_T(j)$, signal MET balanced by $p_T(j)$

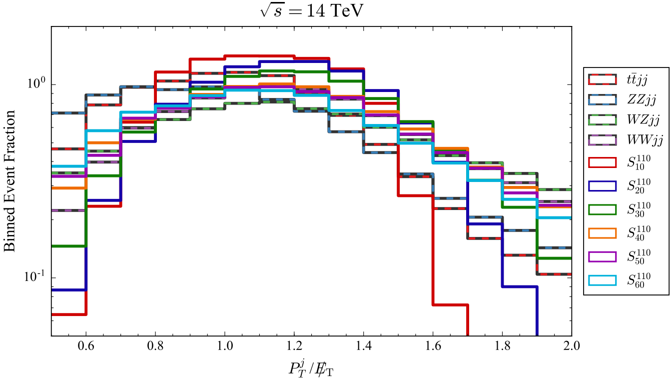

Figure: $0.8 < p_T(j)/\not{E}_T < 1.8$ cut for larger mass differences

$ZZ \to \ell^+\ell^-\nu\bar{\nu}$ has leptons recoiling against MET

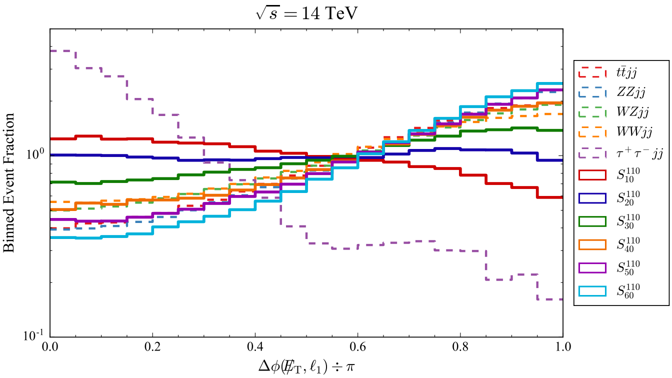

Figure: $\Delta\phi(\not{E}_T, \ell_1) < 0.8\pi$ helps for intermediate mass differences

$W^+W^- \to \ell^+\nu\ell^-\bar{\nu}$ has less anti-collimated leptons

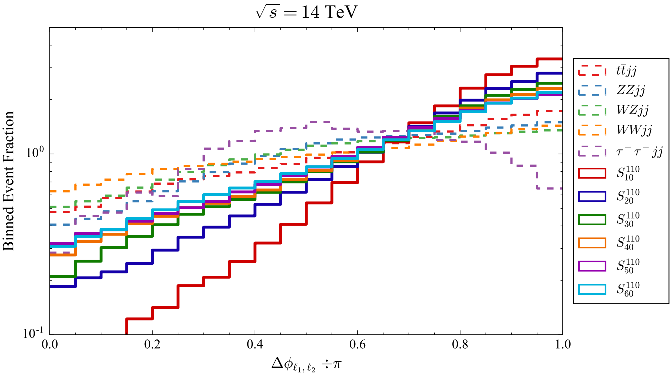

Figure: $\Delta\phi(\ell_1, \ell_2) > 0.5\pi$ suppresses background with lighter parents

$\cos\theta^*_{\ell_1,\ell_2} = \tanh(\Delta\eta_{\ell_1,\ell_2}/2)$ depends on parents' spin

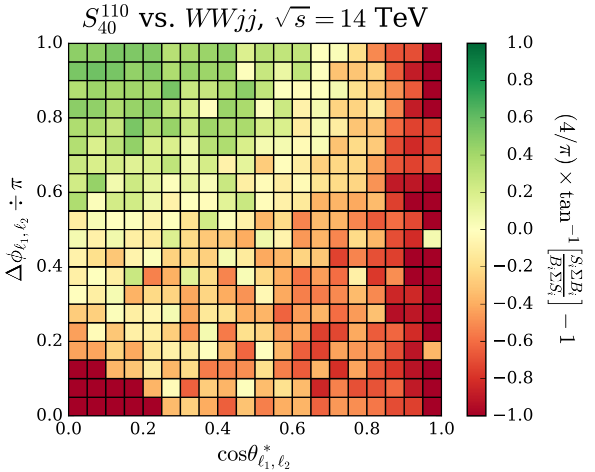

Figure: $\cos\theta^*_{\ell_1,\ell_2} < 0.5\pi$ suppresses background with spin-1 parents

Constraints applied to new MSSM paradigm

LHC can probe compressed sleptons

- $S/B \sim 0.3$ with $\sim 3\sigma$ at $300\ \mathrm{fb}^{-1}$ for $m_{\tilde{\mu}} = 110\,\mathrm{GeV}$
- Scaling up to $m_{\tilde{\mu}} = 160\,\mathrm{GeV}$, $S/B \sim 0.2$ with $\sim 2\sigma$
- Discovery potential with smaller Δm at $300\ \mathrm{fb}^{-1}$ due to more refined angular cuts
- For more on bino DM, see Fukushima et. al. 1406.4903

Light squark co-annihilation

- need $\tilde{q}\chi$ and $\tilde{q}\tilde{q}$ inital states to deplete relic density
- small mixing angle requires more general treatment of direct detection
- velocity suppressed or SD operators can dominate scattering at small α

Thank you!

Relic density for $\tilde{u}_1$

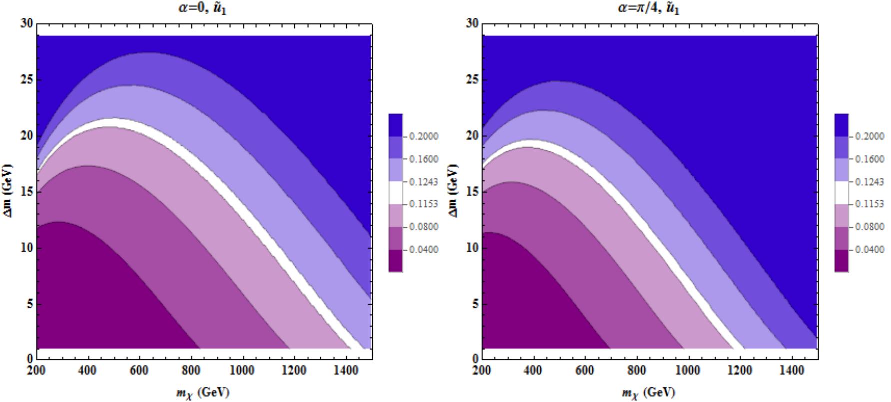

Figure: Relic density contours for benchmarks with light u–type squarks.

Relic density for $\tilde{u}_1 \tilde{d}_1$

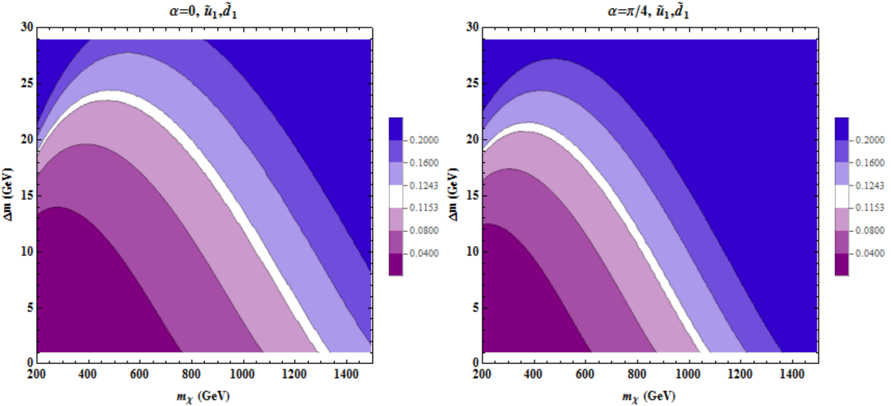

Figure: Relic density contours for benchmarks with light u- and d-type squarks.

Relic density for $\tilde{u}_1 \tilde{u}_2$

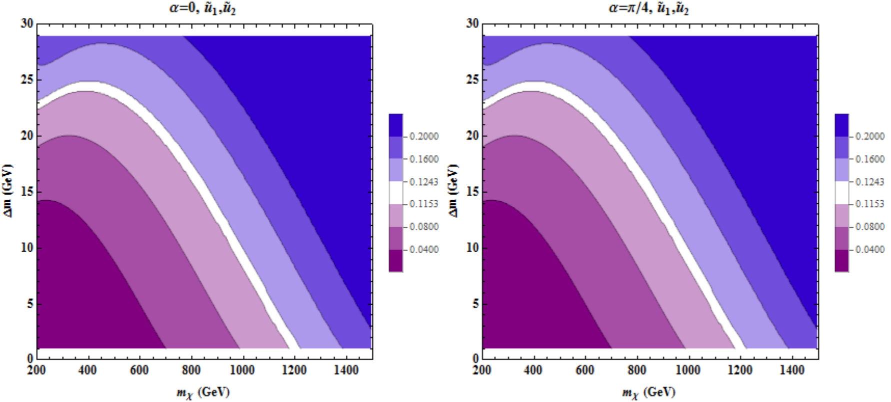

Figure: Relic density contours for benchmarks with two light u–type squarks.

$\tilde{u}_1$ and $\tilde{u}_1 \tilde{u}_2$ in Xenon

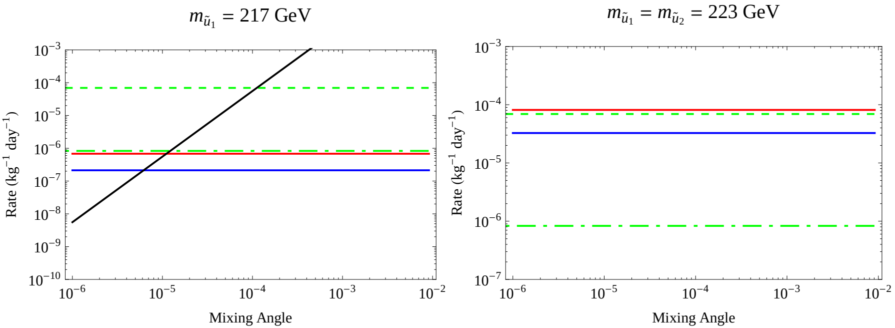

Figure: Event rate in Xenon-based detector as a function of α for $\mathcal{O}_{q1}$, $\mathcal{O}_{q2}$, $\mathcal{O}_{q3}$, $m_\chi = 200\,\mathrm{GeV}$. Also show limits from LUX (dashed) and projections from LZ-7 (dash-dotted).

$\tilde{s}_1$ and $\tilde{u}_1 \tilde{d}_1 \tilde{s}_1$ in Fluorine

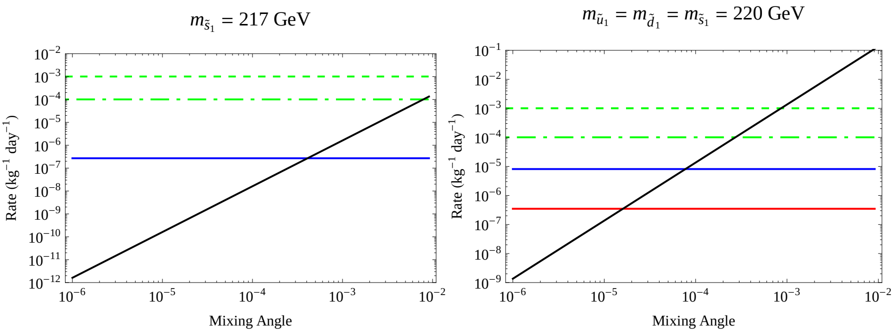

Figure: Event rate in Fluorine-based detector as a function of α for $\mathcal{O}_{q1}$, $\mathcal{O}_{q2}$, $\mathcal{O}_{q3}$, $m_\chi = 200\,\mathrm{GeV}$. Also show limits from PICO-60L (dashed) and projections from PICO-250L (dash-dotted).

$\tilde{u}_1$ and $\tilde{u}_1\tilde{u}_2$ in Fluorine

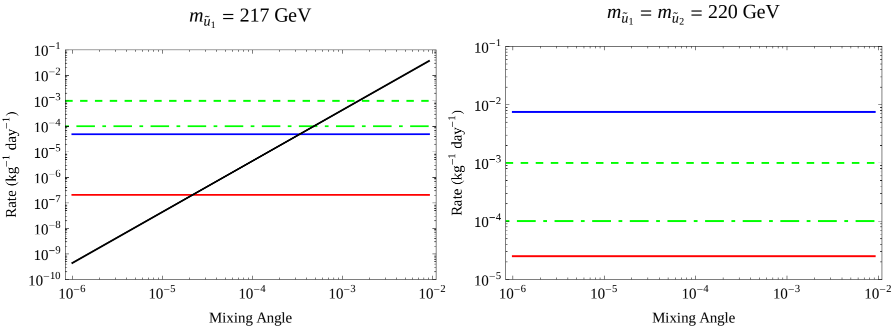

Figure: Event rate in Fluorine-based detector as a function of α for $\mathcal{O}_{q1}$, $\mathcal{O}_{q2}$, $\mathcal{O}_{q3}$, $m_\chi = 200\,\mathrm{GeV}$. Also show limits from PICO-60L (dashed) and projections from PICO-250L (dash-dotted).

Sensitivity of direct detection to SI scattering at LUX

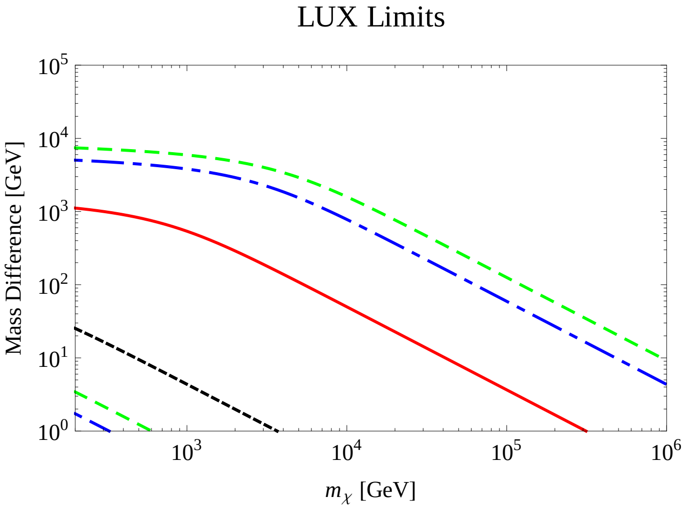

Figure: Projected LUX sensitivity for benchmarks $\tilde{u}_1$, $\tilde{s}_1$, $\tilde{u}_1\tilde{d}_1\tilde{s}_1$, $\tilde{u}_1\tilde{u}_2$.

Dipole moment contributions from L-R slepton mixing

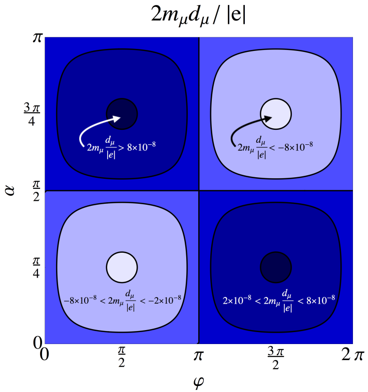

Figure: Muon electric dipole moment contribution assuming smuon mixing with $m_X = 100\,\mathrm{GeV}$, $m_{\tilde{\mu}_1} = 120\,\mathrm{GeV}$ and $m_{\tilde{\mu}_2} = 300\,\mathrm{GeV}$. All unconstrained.

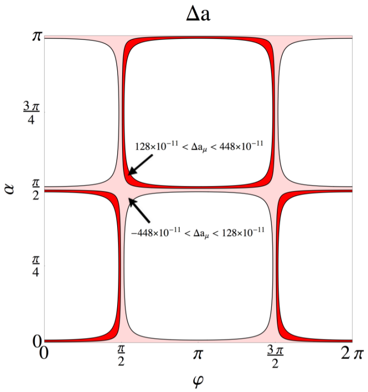

Figure: Muon magnetic dipole moment contribution either fully accounting for measured value (red) or only similar in magnitude (pink).

$M_{\tau\tau}$ supresses $Z \to \tau\bar{\tau}$

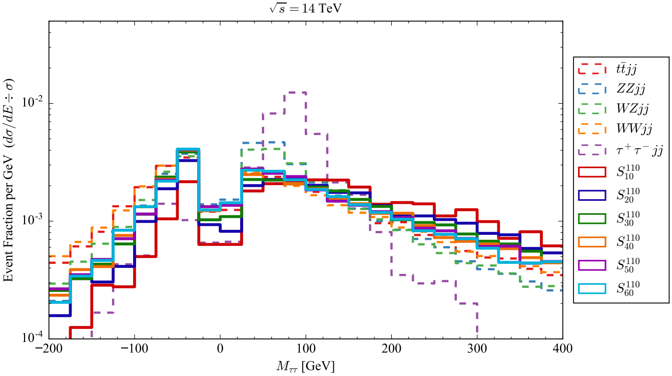

MET cut helps $t\bar{t}$ background

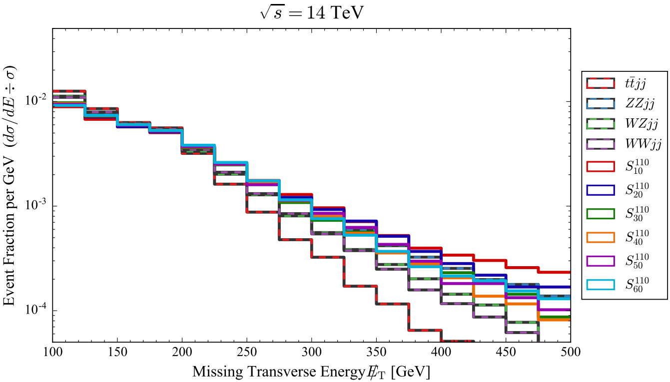

Window cut around on $m_{\ell\ell}$ around m_Z

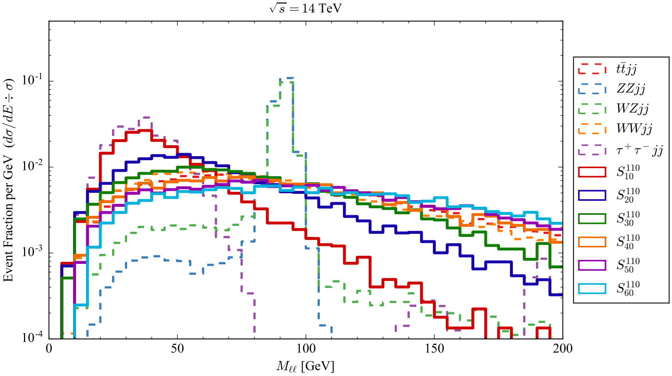

Leading lepton p_T

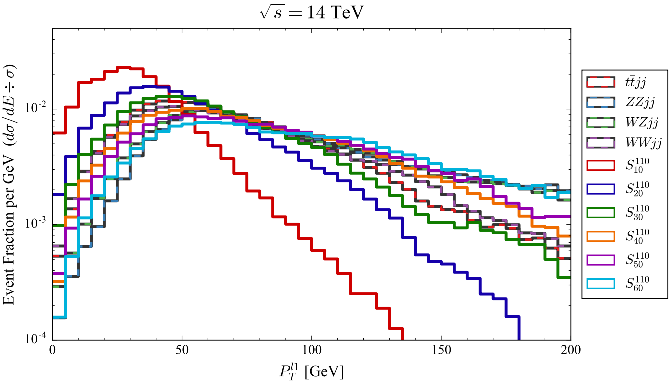

Subleading lepton p_T

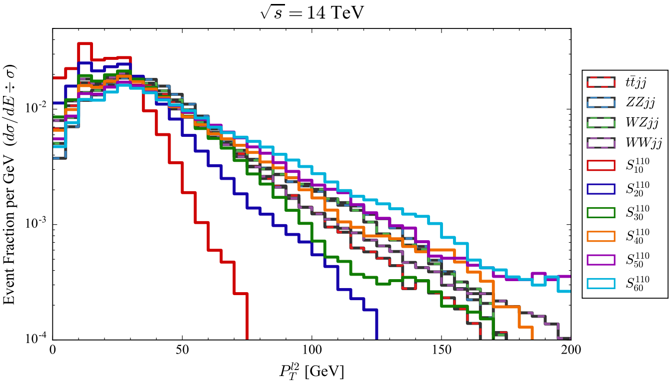

Primary and secondary cuts

Selection	$ZZjj$	$WZjj$	$WWjj$	S^{110}_{30}	S^{110}_{40}	S^{110}_{50}
Matched Production	1.3×10^4	4.2×10^4	9.5×10^4	1.9×10^2	1.9×10^2	1.9×10^2
τ-veto	1.2×10^4	4.0×10^4	8.9×10^4	1.9×10^2	1.9×10^2	1.9×10^2
OSSF muon	3.2×10^2	5.8×10^2	5.1×10^2	8.1×10^1	8.8×10^1	8.9×10^1
only 1J $P_T > 30$	9.4×10^1	1.5×10^2	1.1×10^2	1.6×10^1	1.7×10^1	1.7×10^1
Jet b-veto	8.0×10^1	1.4×10^2	1.1×10^2	1.6×10^1	1.7×10^1	1.7×10^1
$\not{E}_T > 100$ GeV	4.3×10^0	7.8×10^0	1.7×10^1	2.5×10^0	3.4×10^0	3.8×10^0
Jet $P_T > 100$ GeV	1.4×10^0	4.0×10^0	1.0×10^1	1.8×10^0	1.9×10^0	1.8×10^0
$m_{\ell\ell} \notin M_Z \pm 10$ GeV	1.0×10^{-1}	1.0×10^0	8.9×10^0	1.6×10^0	1.6×10^0	1.5×10^0
$m_{\tau\tau} > 175$ GeV	2.0×10^{-2}	3.3×10^{-1}	4.5×10^0	9.3×10^{-1}	9.3×10^{-1}	9.3×10^{-1}
$\not{E}_T > 175$ GeV	8.3×10^{-3}	9.9×10^{-2}	1.3×10^0	3.5×10^{-1}	3.1×10^{-1}	3.2×10^{-1}
Jet $P_T > 175$ GeV	6.6×10^{-3}	8.7×10^{-2}	1.2×10^0	3.3×10^{-1}	2.6×10^{-1}	2.6×10^{-1}

Tertiary cuts targeted at larger mass gaps

Selection	$ZZjj$	$WZjj$	$WWjj$	S_{30}^{110}	S_{40}^{110}	S_{50}^{110}
$M_{T2}^{WW} < 1$ GeV	3.9×10^{-3}	7.0×10^{-2}	8.6×10^{-1}	2.8×10^{-1}	2.1×10^{-1}	2.0×10^{-1}
$0.8 < P_T^j \div \not{E}_T < 1.8\}$	3.9×10^{-3}	5.6×10^{-2}	7.5×10^{-1}	2.7×10^{-1}	1.9×10^{-1}	1.7×10^{-1}
$\Delta\phi(\not{E}_T, \ell_1) \div \pi < 0.8$	3.9×10^{-3}	5.4×10^{-2}	7.2×10^{-1}	2.6×10^{-1}	1.9×10^{-1}	1.6×10^{-1}
$\Delta\phi(\ell_1, \ell_2) \div \pi > 0.5$	2.7×10^{-3}	3.1×10^{-2}	5.6×10^{-1}	2.0×10^{-1}	1.6×10^{-1}	1.2×10^{-1}
$P_T^{\ell 2} > 40$ GeV	0	1.1×10^{-2}	2.3×10^{-1}	9.4×10^{-2}	8.7×10^{-2}	8.4×10^{-2}
Events at $\mathcal{L} = 300\ \mathrm{fb}^{-1}$	0.0	3.4	68.5	28.2	26.1	25.2
$S \div B$	-	-	-	0.34	0.31	0.30
$S \div \sqrt{B}$	-	-	-	3.1	2.9	2.8
Poisson Significance	-	-	-	3.2	3.0	2.9

WIMP miracle predicts new physics at the weak scale

Stable, thermally produced particle will freeze out with relic abundance

$$\Omega_X \sim 1/\langle \sigma_A v \rangle$$

largely independent of DM mass, m_X

Assuming a weak coupling, dimensioanlly, the cross section

$$\langle \sigma_A v \rangle \sim \frac{g_{weak}^4}{m_X^2}(1 \; or \; v^2)$$

$m_X \sim m_{weak}$ will yield the correct Ω_{DM} for s- or p-wave annihilation

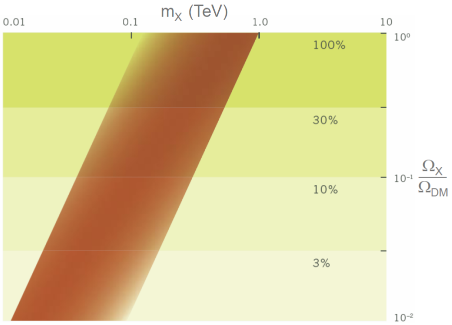

Figure: See Feng 1003.0904.

Weak scale DM motivated by new physics models

Stabilize gauge hierarchy problem → new weak scale particles

- Lightest new particle protected by discreet symmetry
- Provides WIMP candidate

Neutralino in MSSM

- Mixture of neutral gauginos and higgsinos
- SM interactions depend on specific model
- mSUGRA tightly constrained

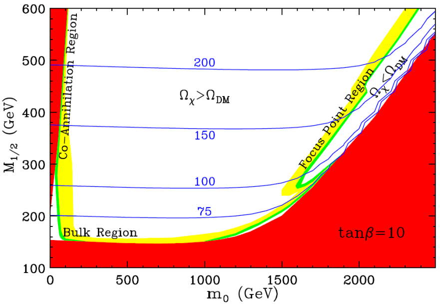

Figure: Cosmologically preferred mSUGRA regions are in green with $A_0 = 0$ and $\mu > 0$. Blue contours denote neutralino masses, see Feng 1003.0904.

MSSM parmeter space decouples into 3 sectors

- *Heavy sector*: Choose μ, heavy squark masses, and top trilinear couplings to obtain a SM Higgs. Decouple M_2, M_3 etc. to satisfy LHC.
- *Relic Density sector*: Choose slepton masses and mixings to achieve the dark matter relic abundance. Alternatively, the abundance may be achieved via coannihilations with squarks.
- *Direct Detection sector*: For a given bino mass, neutralino-nucleon elastic scattering cross sections are determined by the light squark masses and mixings.

PDF suppression of 2nd generation squark production

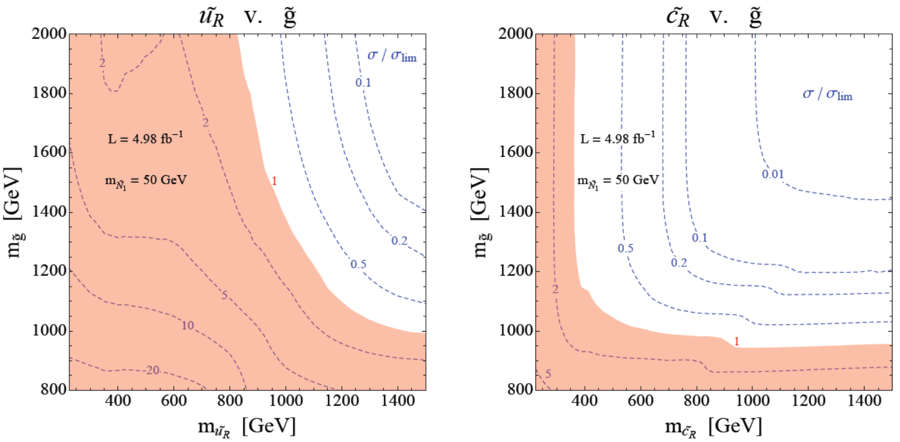

Figure: As $m_{\tilde{g}}$ falls, t-channel gluino exchange becomes important, see Mahbubani et. al. 1212.3328.

Scattering through scalar exchange in non-relativistic limit

$$\sigma^N_{SI} = \frac{\mu_p^2}{32\pi(2J_X+1)} \sum_{spins} \left| \sum_q \frac{B^N_q}{m_X m_q} \mathcal{M}_{Xq\to Xq} \right|^2$$

$$B^N_q = \langle N|\bar{q}q|N\rangle = m_N\ f^N_q/m_q$$

$$B^p_u = B^n_d = \tilde{\Sigma}_{\pi N}\left[1+(1-y)\left(\frac{z-1}{z+1}\right)\right]$$

$$B^p_d = B^n_u = \tilde{\Sigma}_{\pi N}\left[1-(1-y)\left(\frac{z-1}{z+1}\right)\right]$$

$$B^p_s = B^n_s = \tilde{\Sigma}_{\pi N}\, y,\ \ \Sigma_{\pi N} = (m_u+m_d)\tilde{\Sigma}_{\pi N}$$

Largest uncertainty from strangeness content of nucleon $y = 1 - \sigma_0/\Sigma_{\pi N}$

$\Sigma_{\pi N} \sim 59\,\mathrm{MeV}$ can be determined from π-N scattering. $z \simeq 1.49$ and σ_0 can be fit from baryon octet mass differences in chiral pert. theory

Can also calculate σ_0 on the lattice and predict small $\Sigma_{\pi N}$

	$y \to 0$	$y = 0.06$	$y \to 1$
$B_u^p = B_d^n$	9.95 (7.59, 12.2)	9.85 (7.51, 12.1)	8.31 (6.34, 10.3)
$B_d^p = B_u^n$	6.67 (5.09, 8.38)	6.77 (5.17, 8.46)	8.31 (6.34, 10.3)
$B_s^p = B_s^n$	0	0.499 (0.380, 0.617)	8.31 (6.34, 10.3)

Table: Can end up with either small $\sigma_0 \lesssim \Sigma_{\pi N}$ or $\sigma_0 \sim \Sigma_{\pi N}$. We assume the central value for $\Sigma_{\pi N}$ of 59 MeV, with the numbers in parentheses indicating the 2σ range for $\Sigma_{\pi N}$ (45 MeV, 73 MeV), see Alarcon, Camalich, Oller 1110.3797.

$$B^N_{q=c,b,t} = \frac{2}{27}\frac{m_N}{m_q} f^N_g, \;\; f^N_g = 1 - \sum_{q=u,d,s} f^N_q$$

Quark loops could couple heavy flavor squarks to gluon content in nucleon

Recall, for squark mixing, we have $\mathcal{M}_{Xq\to Xq} \sim m_q$, so $q = c, b, t$ contributions to σ^N_{SI} will be suppressed by m_q^{-2} without MFV couplings.

Calculate cross section and check dipole moments

$$\sigma_{SI}^N = \frac{\mu_p^2}{4\pi} \left\{ \sum_q g^2 Y_L Y_{Rq} \sin(2\phi_{\tilde{q}}) \left[\frac{1}{(m_{\tilde{q}_1}^2 - m_X^2)} - \frac{1}{(m_{\tilde{q}_2}^2 - m_X^2)} \right] B_q^N \lambda_q \right\}^2$$

where λ_q accounts for running from the weak scale. For $m_X \ll m_{\tilde{q}_1} \ll m_{\tilde{q}_2}$

$$\frac{\Delta a}{m_q} \sim \frac{m_X}{16\pi^2 m_{\tilde{q}_1}^2} g^2 Y_L Y_{Rq} \sin(2\phi_{\tilde{q}})$$

$$\sigma_{SI}^N \sim (1.1 \times 10^9 \ \mathrm{pb\,GeV}^2) \left(\sum_q \frac{\Delta a_q}{m_q} \frac{B_q^N}{0.5} \right)^2 \left(\frac{m_X}{50 \ \mathrm{GeV}} \right)^{-2}$$

Direct detection already rules out models with $\Delta a_q (\mathrm{GeV}/m_q) \gtrsim 10^{-9}$

No contribution to quark EDM and quark MDM limits are relatively weak

LEP constrains current quark moments by checking Γ_Z contributions and LHC constrains chromomagnetic moments; most stringent $\Delta a_q \lesssim 10^{-5}$

Assume $m_X = 50$ GeV, maximal mixing and minimal B_s^N

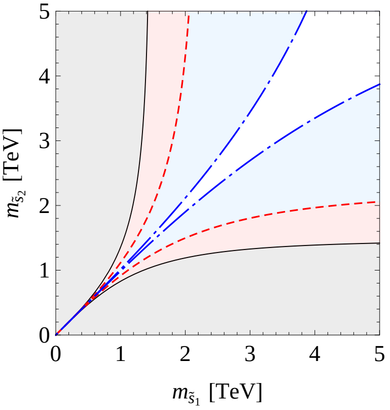

Figure: The grey region is ruled out by **LUX**, the red region could be ruled out by 300 days of LUX data and the blue region could be probed by LZ-7.

Direct detection with decoupled $m_{\tilde{s}_2}$ and minimal B_s^N

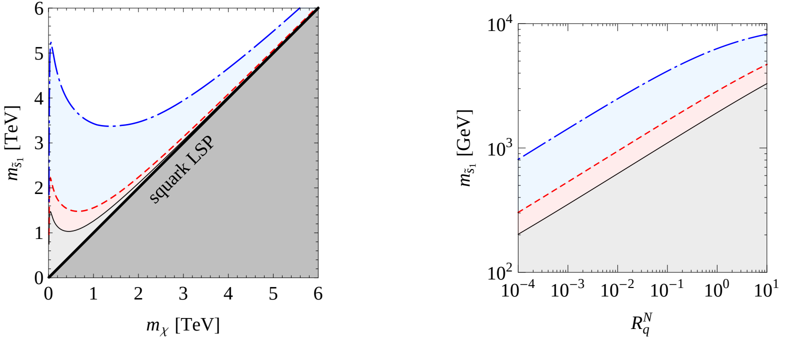

Figure: Sensitivity in the $(m_X, m_{\tilde{s}_1})$ plane assuming maximal mixing (left) and $(R_s^N, m_{\tilde{s}_1})$ plane with $R_q^N \equiv Y_{Rq}^2 \sin^2(2\phi_{\tilde{q}})(B_q^N)^2\lambda_q^2$ and $m_X = 50\ \mathrm{GeV}$ (right).

$$\sigma_{SI}^N \sim \frac{\mu_p^2 R_q^N}{(m_{\tilde{q}_1}^2 - m_X^2)^2}$$

- Enhanced sensitivity near $m_\chi \simeq m_{\tilde{q}_1}$
- Squark mass reach comperable to LHC

Uncertainty in SI scattering due to strangeness content

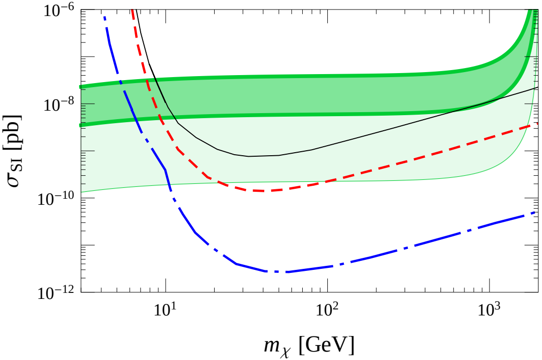

Figure: Sensitivity in the $(m_{\tilde{\chi}}, \sigma^N_{SI})$ plane with with $m_{\tilde{s}_1} = 2$ TeV and maximal mixing. The dark green band indicates the predicted SI-scattering cross section for $\sigma_0 = 27$ MeV and allowing the full 2σ range for $\Sigma_{\pi N}$ of 45 MeV to 73 MeV.